

Photon blockade in a bi-mode nonlinear nano-cavity embedded with a quantum-dot

Xinyun Liang, Zhenglu Duan,* and Qin Guo, Shengguo Guan, Min Xie, Cunjin Liu
College of Physics and Communication Electronics, Jiangxi Normal University, Nanchang 330022, China

We study the interaction between a quantum-dot and a bi-mode micro/nano- optical cavity composed of second-order nonlinear materials. Compared with the Jaynes-Cummings (J-C) model, except for a coherent weak driving field, a strong pump light illuminates the two-mode optical cavity. Analytical results indicate that the model exhibits abundant non-classical optical phenomena, such as conventional photon blockade induced by the nonlinear interaction between polaritons. It constitutes unconventional photon blockade induced by quantum interference due to parametric driving. We compare the photon statistical properties and average photon number of the proposed model, J-C model, and double-mode driven optical cavity under the same parameters and the proposed model can obtain stronger antibunching photons and higher average photon number.

I. INTRODUCTION

Nonclassical light generation is an important objective in the fields of quantum optics, quantum information, and quantum computation[1–5]. Intensity fluctuation of the light field can be used to identify the quantumness of light, e.g., $g^{(2)}(0) \geq 1$ represents classical light, whereas $g^{(2)}(0) < 1$ denotes nonclassical light. Photon blockade (PB) is considered an important mechanism to generate nonclassical light. When a coherent laser imprints on a nonlinear quantum optical cavity, a photon existing in the cavity may blockade other photons entering the cavity because of the strong interaction between photons[6]. In the limit of strong nonlinearity, the PB effect could be a good mechanism to generate single photons with perfect purity. The PB effect, which is based on strong nonlinearity, has been studied in many quantum systems, such as atom-cavity system[7], single quantum-dot cavity system[8, 9], $\chi^{(2)}$ nonlinear doubly resonant nanocavity system[10], and opto-mechanical systems[11–13].

Recently, researchers have found that a strong antibunching light can be obtained by the quantum interference of different driven-dissipative pathways in a quantum optics system[14]. Contrary to the strong linearity induced PB, weak nonlinearity helps realize the photon antibunching induced by quantum destructive interference. To differentiate the photon antibunching processes induced by different physical mechanisms, the antibunching induced by strong nonlinear interaction between photons is referred to as conventional photon blockade (CPB), whereas that by the quantum interference is termed unconventional photon blockade (UCPB). Since its proposition, many theoretical and experimental works have focused on UCPB in different systems, such as coupled nonlinear cavities[14], superconducting qubit microwave cavity[15] and opto-mechanical systems, two coupled nonlinear single-mode cavity system[16], and $\chi^{(2)}$ nonlinear coupled or doubly-resonant cavity system[17, 18].

Currently, studies have found that the quantum interference phenomenon can be used to enhance the CPB, and consequently the purity of the generated single-photon[19]. In addition, we note that CPB and UCPB can coexist in the same quantum optics system[19, 20], which is helpful in further understanding the physical mechanism behind CPB/UCPB.

In this study, we propose a model to generate strong PB with a single quantum-dot (QD) that is strongly coupled to a bi-mode nonlinear nanocavity, which is filled with $\chi^{(2)}$ medium. The proposed model can be considered a composite model of the J-C model and the bi-mode driven nonlinear optical cavity. Studies have indicated that CPB and UCPB exist in the Jaynes-Cummings (J-C) model with strong coupling and the bi-mode driven nonlinear optical cavity[17, 18]. Thus, we expect CPB induced by strong nonlinear interaction and UCPB induced by quantum interference to simultaneously appear in the proposed model, when the system is in the strong coupling regime. By studying the proposed model, we find that strong UCPB appears in the red atomic detuning region, which does not occur in the J-C model. Comparing the J-C model with bi-mode driven nonlinear nanocavity, more transition pathways from ground to two-photon states in the proposed model make the quantum statistics of the photons more complicated.

The remainder of this paper is organized as follows. In Section II, we present the effective Hamiltonian to describe the proposed system. In Section III, we study the physical mechanism of PB using the wavefunction approach, and provide the optimal conditions for strong photon antibunching via second-order correlation function. In addition, we

*Electronic address: duanzhenglu@jxnu.edu.cn

theoretically study the relationship between the PB effect in our model and J-C and empty cavity models using the quantum interference transition paths. In Section IV, we provide the numerical results of a second-order correlation function and compare them with the analytical results. Finally, we conclude this paper in Section V.

II. MODEL

The proposed model is depicted in Fig. 1(a) with a single QD embedded in a doubly resonant nonlinear nanocavity made of $\chi^{(2)}$ material. For $\chi^{(2)}$ nonlinearity, the fundamental and the second harmonic modes are coupled together and mediate the conversion of one photon in second-harmonic mode to two photons in fundamental mode. In the rotating frame of the weak driving and strong pump lights defined by $U(t) = \exp[-i\omega_d(\sigma_+\sigma_- + \hat{a}^\dagger\hat{a})t - i\omega_p\hat{b}^\dagger\hat{b}t]$, the interaction Hamiltonian of the system is given by,

$$H = \delta\sigma_+\sigma_- + \Delta_a\hat{a}^\dagger\hat{a} + \Delta_b\hat{b}^\dagger\hat{b} + E(\hat{a} + \hat{a}^\dagger) + F(\hat{b} + \hat{b}^\dagger) + g(\sigma_+\hat{a} + \hat{a}^\dagger\sigma_-) + \chi(\hat{b}^\dagger\hat{a}^2 + \hat{a}^{\dagger 2}\hat{b}), \quad (1)$$

where $\sigma_+(\sigma_-)$ represents the raising and lowering operators of the QD at the transition frequency ω_0 , and $\hat{a}^\dagger(\hat{a})$ represents the creation and annihilation operators of the fundamental mode with the resonance frequency ω_a . Further, $\hat{b}^\dagger(\hat{b})$ represents the creation and annihilation operators of the second harmonic mode with the resonance frequency ω_b . The driving field with the resonance frequency ω_d and strength E acts in the fundamental mode. The second harmonic mode is driven by the pumping field with the resonance frequency ω_p and strength F . Further, g is defined as the coupling between the fundamental mode and the QD, and χ is the parametric gain that denotes the coefficient of second-order nonlinear interactions. In addition, $\delta = \omega_0 - \omega_d$ ($\Delta_a = \omega_a - \omega_d$) denotes the detuning between the QD (fundamental mode) and the driving light, and $\Delta_b = \omega_b - \omega_p$ denotes the detuning between the second harmonic mode and the pumping light.

Considering that the pumping light is very strong and the depletion by the second harmonic mode is negligible, the equation of motion for the operator \hat{b} can be approximately expressed as $id\hat{b}/dt = [\hat{b}, H] \simeq (\Delta_b - i\kappa_b/2)\hat{b} + F$, where κ_b is the decay rate of the second harmonic mode. By allowing the operator \hat{b} to be time-independent, we obtain $\hat{b} \simeq F/(i\kappa_b/2 - \Delta_b)$. Substituting the expression of the operator \hat{b} in Eq. (1), the effective Hamiltonian can be reduced as follows,

$$H_{eff} = \delta\sigma_+\sigma_- + \Delta_a\hat{a}^\dagger\hat{a} + g(\sigma_+\hat{a} + \sigma_-\hat{a}^\dagger) + E(\hat{a} + \hat{a}^\dagger) + U(\hat{a}^2 + \hat{a}^{\dagger 2}), \quad (2)$$

with the effective parametric gain $U = F\chi/\sqrt{\Delta_b^2 + \kappa_b^2/4}$. Here, we assumed real parametric gain via a well-chosen relative phase of the pump field. Further, Eq. (2) indicates that the current model can be considered as a J-C model with a parametric gain or bi-mode nonlinear cavity embedded with a single QD.

Unlike the J-C model, our scheme with the Hamiltonian in Eq. (2) has an additional parametric gain. In addition, when $g = 0$, our scheme can be regarded as a bi-mode driven optical cavity, which has been studied in Ref. [18] in which the PB arises only from the quantum interference. As discussed below, we find the optimal condition of photon antibunching in terms of effective parametric gain and coupling strength based on the effective Hamiltonian H_{eff} , and analyze the difference between the features of the PB effect and the J-C model and the bi-mode driven optical cavity.

III. OPTIMAL CONDITION FOR PHOTON ANTIBUNCHING

It is known that $g^{(2)}(0) < 1$ implies The anti-bunched distribution of photons. In this section, we analytically derive the optimal conditions for strong photon antibunching using the wavefunction approach in Ref. [10, 20–22].

In a weak driving limit, under the assumption that higher photon excitation states have a very low population, the wavefunction of the system is written as,

$$|\Psi\rangle = C_{0,g}|0, g\rangle + C_{0,e}|0, e\rangle + C_{1,g}|1, g\rangle + C_{1,e}|1, e\rangle + C_{2,g}|2, g\rangle, \quad (3)$$

where the coefficients $C_{n,g}$ and $C_{n,e}$ denote the amplitudes of the system in the states $|n, g\rangle$ and $|n, e\rangle$, respectively. The state $|n, g\rangle$ (or $|n, e\rangle$) indicates that the system has n ($n = 0, 1, 2$) photons of fundamental mode and is in the ground state $|g\rangle$ (or excited state $|e\rangle$) of the atom. By using the wavefunction, we obtain $g^{(2)}(0) \simeq 2|C_{2,g}|^2/|C_{1,g}|^4$.

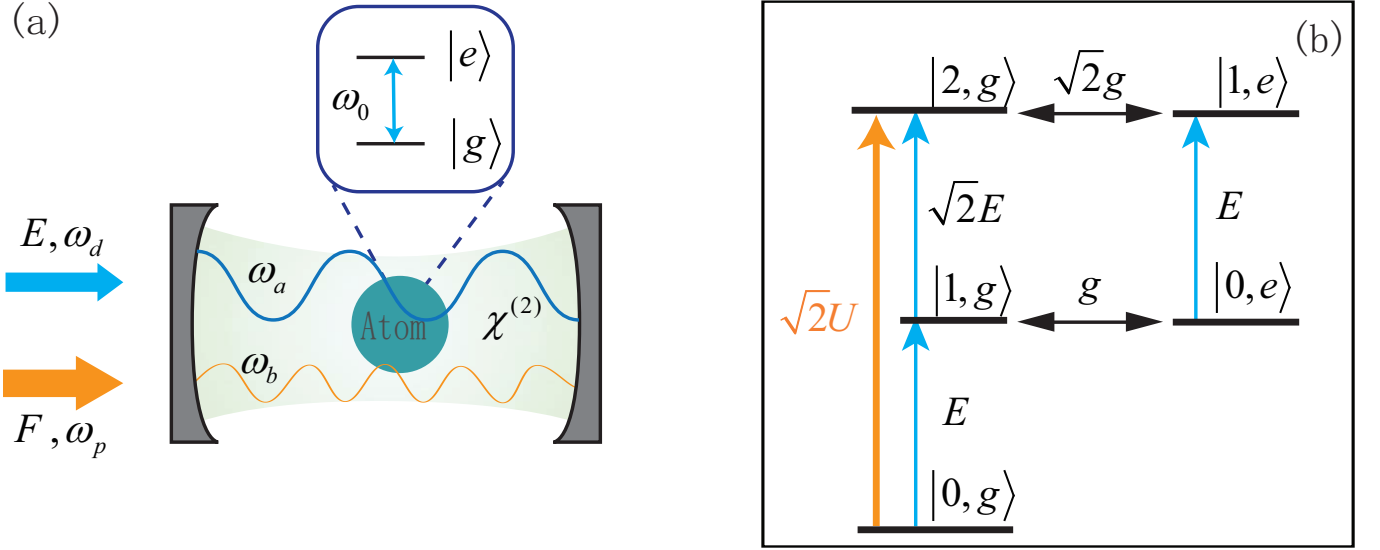


FIG. 1: (Color online) (a) Schematic showing a quantum dot embedded in a nonlinear nanocavity made of $\chi^{(2)}$ medium. (b) Energy-level diagram showing the transition between zero-, one-, and two- photon states and the transition paths leading to quantum interference for obtaining antibunching photons.

Now, substituting the wavefunction (3) and the effective non-Hermitian Hamiltonian in the Schrodinger equation, a set of equations for coefficients can be given as follows:

$$i\dot{C}_{0,e} = gC_{1,g} + \delta' C_{0,e}, \quad (4)$$

$$i\dot{C}_{1,g} = EC_{0,g} + gC_{0,e} + \Delta'_a C_{1,g}, \quad (5)$$

$$i\dot{C}_{1,e} = \sqrt{2}gC_{2,g} + (\Delta'_a + \delta') C_{1,e} + EC_{0,e}, \quad (6)$$

$$i\dot{C}_{2,g} = \sqrt{2}EC_{1,g} + \sqrt{2}gC_{1,e} + 2\Delta'_a C_{2,g} + \sqrt{2}UC_{0,g}. \quad (7)$$

Here, we defined $\delta' = \delta - i\gamma/2$ and $\Delta'_a = \Delta_a - i\kappa/2$ with γ and κ being the decay rate of the QD and leakage rate of the fundamental mode of the nanocavity, respectively. Using the above set of equations, we can obtain the coefficients $C_{1,g}$ and $C_{2,g}$, when the system is in the steady state ($\{\dot{C}_{n,e}, \dot{C}_{n,g}\} = 0$), as follows:

$$C_{1,g} = \frac{E\delta'}{g^2 - \delta'\Delta'_a}, \quad (8)$$

$$C_{2,g} = \frac{E^2 [g^2 + \delta'(\Delta'_a + \delta')] - U(\delta'\Delta'_a - g^2)(\Delta'_a + \delta')}{\sqrt{2}[\Delta'_a(\Delta'_a + \delta') - g^2](\delta'\Delta'_a - g^2)}. \quad (9)$$

Finally, the second order correlation function in the weak driving limit can be presented:

$$\begin{aligned} g^{(2)}(0) &\simeq \frac{2|C_{2,g}|^2}{|C_{1,g}|^4} \\ &= \left| g^2 - \delta'\Delta'_a \right|^2 \left| \frac{E^2 g^2 + (\Delta'_a + \delta')(E^2 \delta' - \delta' U \Delta'_a + U g^2)}{E^2 \delta'^2 (\Delta'_a (\Delta'_a + \delta') - g^2)} \right|^2. \end{aligned} \quad (10)$$

Clearly, Eq. (10) indicates that, in the limit of strong coupling strength, i.e., $g \gg (\gamma, \kappa)$, when $\Delta_a \delta = g^2$ or $g^2 = \delta(\Delta_a + \delta)(U\Delta_a - E^2)/(E^2 + U(\Delta_a + \delta))$, $g^{(2)}(0)$ takes local minimal values. We further discuss the second order correlation function for both these cases, where we first consider the case $\Delta\delta = g^2$. Under this condition, the second order correlation takes a local minimum value as follows,

$$g^{(2)}(0) \approx \frac{\gamma^2}{g^2} \left(1 + \frac{\gamma^2 U^2}{E^4} \right). \quad (11)$$

It is noted that, if the effective parametric gain U is significantly smaller than the driving strength E , $g^{(2)}(0) \ll 1$ corresponds to strong photon antibunching; therefore, $\Delta\delta = g^2$ is a local optimal condition for photon antibunching. The physical mechanism behind photon antibunching is that the strong interaction between the photons blockades more photons entering the nanocavity at the same time, which is the same as the case of photon blockade in the J-C model. The optimal condition indicates that the strong antibunching induced by the strong nonlinearity only occurs when the signs of atomic and cavity detuning processes are the same.

On the contrary, if $C_{2,g} = 0$, the second order correlation function vanishes, i.e., $g^{(2)}(0) = 0$. Based on Eq. (??) we can arrive at the following condition to satisfy $C_{2,g} = 0$:

$$g^2 = \frac{U\Delta'_a - E^2}{E^2 + U(\Delta'_a + \delta')} \delta' (\Delta'_a + \delta'). \quad (12)$$

It is noted that Eq. (12) is another local optimum condition for strong photon antibunching. Unlike that in the strong coupling case, the physical mechanism of the strong antibunching effect in this scenario originates from quantum interference. From the energy level diagram (Fig. 1(b)), one observes that three different transition paths are available to the two-photon state $|2, g\rangle$: $\chi^{(2)}$ nonlinearity interaction leading $|0, g\rangle \xrightarrow{\sqrt{2}U} |2, g\rangle$; atomic-cavity coupling inducing $|1, e\rangle \longleftrightarrow |2, g\rangle$, and external field driving inducing $|1, g\rangle \longleftrightarrow |2, g\rangle$. If the system parameters satisfy the optimal condition, the total transition results in a nearly perfect destructive interference and a nearly vanishing population of the two-photon state $|2, g\rangle$. Moreover, we can find that, when $U \rightarrow 0$, our model reduces to J-C model, and the optimal condition in Eq. (12) reduces to $g^2 = -\delta(\delta + \Delta_a)$, which is consistent with the optimal condition for UCPB in the J-C model [20]. On the other hand, when $g \rightarrow 0$, the system degenerates into a double-mode driven nonlinear optical cavity, and the optimal condition (12) becomes $E^2 = U\Delta_a$, which is similar to the results of Ref. [18].

IV. NUMERICAL RESULTS

We present the numerical results of the equal time second-order correlation function $g^{(2)}(0)$ in this section to illustrate the photon statistics of the fundamental mode. In numerical calculation, we evaluate $g^{(2)}(0) = \text{Tr}(\rho a^\dagger a^\dagger a a) / \text{Tr}(\rho a^\dagger a)^2$ by solving the master equation, when the system is in the steady state; the master equation is defined as $\partial\rho/\partial t = -i[H_{eff}, \rho] + \kappa L[\hat{a}]\rho/2 + \gamma L[\sigma_-]\rho/2$ with $L[\hat{o}]\rho = 2\hat{o}\rho\hat{o}^\dagger - \hat{o}^\dagger\hat{o}\rho - \rho\hat{o}^\dagger\hat{o}$, denoting Lindblad equations. Considering the system is in strong coupling, and taking $g = 20\gamma$ as an example, we numerically study and plot the dependence of the second order correlation function $g^{(2)}(0)$ on cavity detuning Δ_a and QD detuning δ , as shown in Fig. 2(a). It can be seen from Fig. 2(a) that, when the signs of cavity and QD detunings are the same (both δ and Δ_a are either blue or red), three troughs are present for strong photon antibunching ($g^{(2)}(0) \ll 1$), which are represented by the deep blue region. The expressions of two of these three troughs share the same parametric condition with $\delta\Delta_a = g^2$ (highlighted by red dashed line), which corresponds to the PB induced by strong nonlinear interaction. One red dashed line is located in the first quadrant, and another in the third quadrant, which results are consistent with those discussed in Section III and with the case in a normal two-level atom emitted cavity system[20]. The remaining trough located in the first quadrant, which is indicated by white dashed line with the numerical optimal parametric relation, confirms the analytical results (Eq. (12)). It is noted that the PB induced by quantum interference under this parametric condition-which is an interesting feature in our work-not only originates from the strong nonlinear interaction but also is induced by the quantum interference, when $\{\delta, \Delta_a\} > 0$ with $U \neq 0$. Apparently, one can see that the optimal condition in (12) does not hold, when the cavity and atomic detunings (both in red) are located in the third quadrant, implying that the photons are bunched.

In addition, when the signs of cavity and QD detunings are opposite, $\delta\Delta_a < 0$. It is seen that one trough exists in $g^{(2)}(0) < 1$ for strong antibunching photons, in the second quadrant (QD detuning is represented in red and cavity detuning in blue), indicated by the white dashed line with the optimal parametric condition satisfying Eq. (12), which corresponds to the PB originating from quantum interference. However, for another condition of $\delta\Delta_a < 0$ (QD detunings are represented in blue and cavity detuning in red), located in the fourth quadrant, it is obvious that observing PB is difficult to observe with respect to photon bunching. This scenario is completely different from the cases in the first and the second quadrants, where the PB can be clearly observed.

Then, we plot $g^{(2)}(0)$ as a function of atomic detuning δ in Fig. 2(b). It is seen that, when cavity detuning is in the red region, taking $\Delta_a = -20\gamma$ as an example, only one trough is located at $\delta = -20\gamma$ with red QD detuning; the corresponding optimal value of second correlation function is $g^{(2)}(0) \approx 0.022$. In this case, we found that both the cavity and QD detunings are in red with the optimal parametric condition satisfying $\delta\Delta_a = g^2$, which corresponds to the PB arising from the strong nonlinear interaction. This result indicates that only one feasible method of strong nonlinear interaction is available to observe PB, when $\Delta_a < 0$.

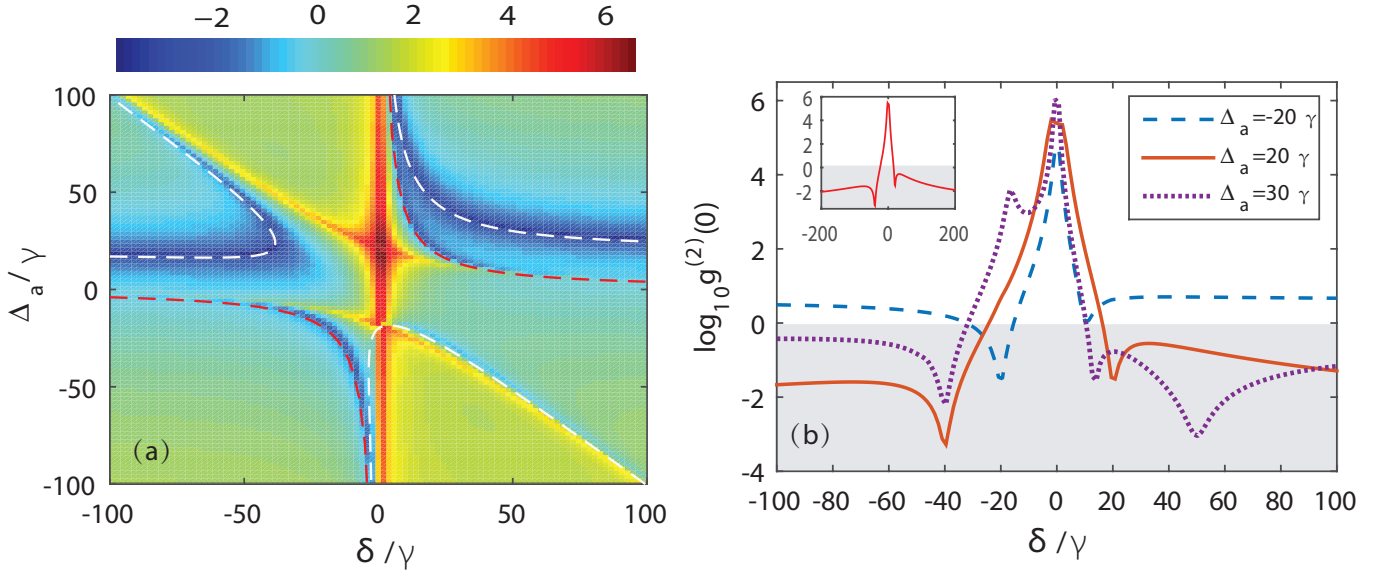


FIG. 2: (Color online) (a) Second-order correlation function $\log_{10} g^{(2)}(0)$ as a function of atomic detuning δ and cavity detuning Δ_a . (b) Cross section of the left panel along δ with cavity detuning $\Delta_a = -20\gamma, 20\gamma, 30\gamma$. Other parameters are taken as $\kappa = \gamma$, $E = 0.1\gamma$, $U = 0.0005\gamma$, $g = 20\gamma$.

Furthermore, when the cavity detuning is red, we take $\Delta_a = 20\gamma, 30\gamma$ as examples. When $\Delta_a = 20\gamma$, i.e., $\Delta_a = E^2/U$, we find that there are only two troughs in $g^{(2)}(0) \ll 1$ for stronger antibunching photons. A trough at $\delta \simeq 20\gamma$, whose parametric condition satisfies $\delta\Delta_a = g^2$, is consistent with the case when $\Delta_a = -20\gamma$, which corresponds to the PB originating from the strong nonlinear interaction, with both cavity and QD detunings being blue. Another trough located at $\delta = -40\gamma = -2E^2/U$, whose optimal parametric condition for strong antibunching is given by Eq. (12), corresponds to the PB caused by quantum interference. A comparison of the values of $g^{(2)}(0)$ in these two troughs indicates that $g^{(2)}(0)$ in $\delta = -40\gamma$ is smaller than $g^{(2)}(0)$ in $\delta = 20\gamma$, implying stronger photon antibunching, when PB is caused by quantum interference. Now, we discuss another case in which $\Delta_a = 30\gamma > E^2/U$; here, one can see that, in addition to $g^{(2)}(0) \ll 1$ for strong antibunching photons at $\delta = -40\gamma, \delta = 50\gamma$ exists, from which the PB originating from quantum interference is observed as well; both the parameters given here satisfy Eq. (12). Unlike the case with $\Delta_a = E^2/U$, two troughs are present from which the PB effect is observed; the PB in both these cases was induced by quantum interference. Apparently another trough is located at $\delta \approx -13.3\gamma$ for the PB effect induced by strong nonlinear interaction. Apart from the above discussion, we can see that $g^{(2)}(0)$ tends to stabilize at $|\delta| > 2E^2/U$, as illustrated in Fig. 2(b) with $\Delta_a = 20\gamma$.

The above discussion clearly indicates that the model proposed in this paper under different parameters can be reduced to a different well-known model. For example, when $U = 0$, our model is reduced to J-C model, and when $g = 0$, it becomes a bi-mode driven optical cavity. To further understand the photon statistical properties of these three models under the same parameters, we plot $g^{(2)}(0)$ with cavity detuning Δ_a in Fig. 3(a) with QD detuning $\delta = 30\gamma$. The red line represents the case where $U = 0$ and $g = 20\gamma$, corresponding to the J-C model. One can see that a trough exists, where the minimum value of $g^{(2)}(0)$ is significantly less than 1, implying a strong photon antibunching. The trough is located at $\Delta_a = 13.3\gamma$. Obviously, the parameter satisfying the optimal relation $\delta\Delta_a = g^2$ and photon antibunching comes from the strong nonlinear interaction. The yellow dashed line indicates the condition of a bi-mode driven optical cavity with the parameters $g = 0$ and $U = 0.0005\gamma$. A highly deep trough is found at $\Delta_a = 20\gamma$, where $g^{(2)}(0) \approx 0.001$, which is greatly lower than that of the J-C model. Now, the parameters satisfy the optimal parametric relation $\Delta_a U = E^2$. Clearly, the strong photon antibunching at the optimal parameter point is caused by quantum interference.

In addition, we study the case with existing parametric gain and a QD in the cavity by setting the parameters as $U = 0.0005\gamma$ and $g = 20\gamma$. Now, the system can be regarded as a composite system of the J-C model and the bi-mode driven optical cavity. The result is represented by the blue dotted line in Fig. 3(a). It is noted that two troughs are present at $g^{(2)}(0) \ll 1$ in the red QD detuning region. The first is located at $\Delta_a = 13.3\gamma$, satisfying the optimal parameter relation $\delta\Delta_a = g^2$. Thus, the physical mechanism of PB arises from the strong nonlinear interaction, similar to the J-C model. This result implies that the parametric gain does not affect the nonlinear interaction between the QD and the fundamental mode of cavity. The second trough is located at $\Delta_a = 37.3\gamma$, which satisfies the optimal parameter relation (12), indicating that quantum interference causes PB. However, the optimal cavity detuning in the

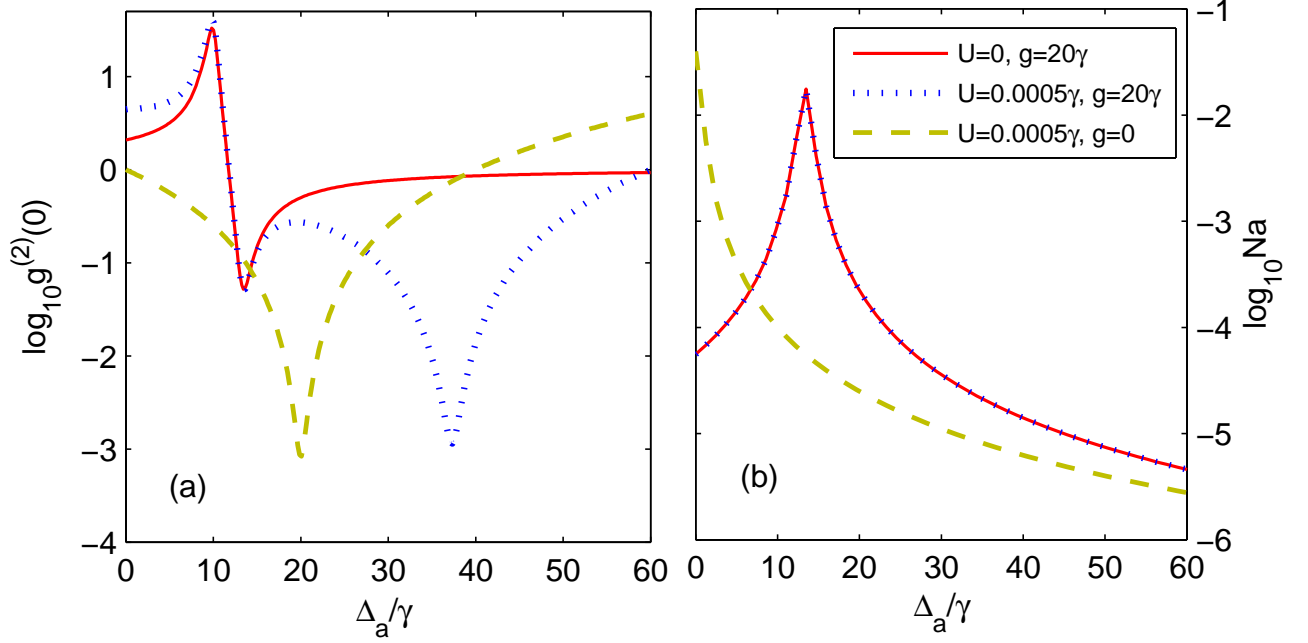


FIG. 3: (Color online) Second-order correlation function $\log_{10} g^{(2)}(0)$ and average photon number $\log_{10} N_a$ as functions of cavity detuning Δ_a with red solid line on $U = 0$ and $g = 20\gamma$, purple dotted line on $U = 0.0005\gamma$ and $g = 20\gamma$, yellow dashed line on $U = 0.0005\gamma$, and $g = 0$ in (a) and (b) respectively. Other parameters are taken as $\kappa = \gamma$, $E = 0.1\gamma$, $\delta = 30\gamma$.

composite system differs from that in the bi-mode driven optical cavity. The principle behind this phenomenon is that, compared with the bi-mode driven optical cavity, three transition paths, rather than two, are involved, resulting in a destructive quantum interference in the composite system, as shown in Fig. 1(b). The above discussion illustrates that the fundamental mode in the proposed composite system has a more comprehensive quantum statistics behavior than that in the J-C mode and the bi-mode driven optical cavity.

Finally, we discuss the influence of quantum interference on the average photon number. The average photon number of the fundamental mode of the cavity is $n_a = \langle a^\dagger a \rangle \simeq |C_{1g}|^2$. Comparing Eq. (8) and Eq. (14) in Ref.[20], one can see that the average photon number in the proposed model is the same as that in the J-C model, which is confirmed by the numerical results in Fig. 3(b) as well. The blue dotted line in Fig. 3 indicates that, for the proposed model, although the quantum interference between the two transition pathways greatly influences the photon statistics and results in a strong photon antibunching around $\Delta_a = 37.3\gamma$, the average photon number remains almost unaffected. Therefore, in the weak driving limit, the average photon number is almost determined by the population of the single-photon state $|1, g\rangle$, and the second order correlation function is approximately proportional to the two-photon state $|2, g\rangle$. The quantum interference affects only the two-photon state $|2, g\rangle$ and therefore the quantum statistics, rather than the average photon number of the fundamental mode. The second order correlation function and the average photon number of the bi-mode driven cavity (yellow dashed lines in Fig. 3) further corroborate this conclusion.

V. CONCLUSION

In this study, we proposed a physical model to realize conventional/unconventional photon blockade in a parametric driven nanocavity embedded with a quantum dot. In the weak driving limit, we used the wave function method to obtain the second-order correlation function expression of the fundamental mode of the nanocavity, and found the optimal parametric conditions to realize strong photon blockade. By analyzing the second order correlation function, we found that conventional and unconventional photon blockades exist simultaneously in the red cavity detuning region. By comparison with the J-C model and the bi-mode driven nanocavity model, we found that the photon blockades originating from strong nonlinearity and quantum interference exist simultaneously in the proposed model. In addition, we found that quantum interference does not influence the average number of photons, whereas it greatly influences the statistical distribution of photons.

Funding Information

National Natural Science Foundation of China (NSFC) (11664014, 11504145, 11964014, and 11364021).

-
- [1] V. Scarani, H. Bechmann-Pasquinucci, N. J. Cerf, M. Dusek, N. Lutkenhaus, M. Peev, The security of practical quantum key distribution, *Rev. Mod. Phys.* **81**, 1301 (2009).
 - [2] E. Knill, R. Laflamme, G. J. Milburn, A scheme for efficient quantum computation with linear optics, *Nature* **409**, 46-52 (2001).
 - [3] P. Kok, W. J. Munro, K. Nemoto, T. C. Ralph, J. P. Dowling, G. J. Milburn, Linear optical quantum computing with photonic qubits, *Rev. Mod. Phys.* **79**, 135 (2007).
 - [4] T. D. Ladd, F. Jelezko, R. Laflamme, Y. Nakamura, C. Monroe, and J. L. O'Brien, Quantum computers, *Nature* **464**, 45-53 (2010).
 - [5] M. A. Nielsen and I. L. Chuang, *Quantum Computation and Quantum Information* (Cambridge University Press, 2010).
 - [6] I. Carusotto, C. Ciuti, Quantum fluids of light *Rev. Mod. Phys.* **85**, 299 (2013).
 - [7] K. M. Birnbaum, A. Boca, R. Miller, A. D. Boozer, T. E. Northup, and H. J. Kimble, Photon blockade in an optical cavity with one trapped atom, *Nature* **436**, 87 (2005).
 - [8] A. Reinhard, T. Volz, M. Winger, A. Badolato, K. J. Hennessy, E. L. Hu and A. Imamoglu, Strongly correlated photons on a chip, *Nature photonics*, **6**, 93-96 (2011).
 - [9] A. Faraon, I. Fushman, D. Englund, N. Stoltz, P. Petro and J. Vuckovic, Coherent generation of non-classical light on a chip via photon-induced tunnelling and blockade, *Nature Phys.* **4**, 859 (2008).
 - [10] A. Majumdar and D. Gerace, Single-photon blockade in doubly resonant nanocavities with second-order nonlinearity, *Phys. Rev. B* **87**, 235319 (2013).
 - [11] X. W. Xu, Y. J. Li, and Y. X. Liu, Photon-induced tunneling in optomechanical systems, *Phys. Rev. A* **87**, 025803 (2013).
 - [12] P. Rabl, Photon blockade effect in optomechanical systems, *Phys. Rev. Lett.* **107**, 063601 (2011).
 - [13] J. Q. Liao and F. Nori, Photon blockade in quadratically coupled optomechanical systems, *Phys. Rev. A* **88**, 023853 (2013).
 - [14] T. C. H. Liew and V. Savona, Single Photons from Coupled Quantum Modes *Phys. Rev. Lett.* **104**, 183601 (2010).
 - [15] A. J. Hoffman, S. J. Srinivasan, S. Schmidt, L. Spietz, J. Aumentado, H. E. Tureci and A. A. Houck, Dispersive Photon Blockade in a Superconducting Circuit, *Phys. Rev. Lett.* **107**, 053602 (2011).
 - [16] H. Flayac and V. Savona, Unconventional photon blockade, *Phys. Rev. A* **96**, 053810 (2017).
 - [17] Y. H. Zhou, H. Z. Shen, and X. X. Yi, Unconventional photon blockade with second-order nonlinearity, *Phys. Rev. A* **92**, 023838 (2015).
 - [18] Y. Y. Yan, Y. B. Cheng, S. G. Guan, D. Y. Yu, and Z. L. Duan, Pulse-regulated single-photon generation via quantum interference in a $\chi^{(2)}$ nonlinear nanocavity, *Opt. Lett.* **43**(20), 5086-5089 (2018).
 - [19] J. Tang, W. D. Geng, X. L. Xu, Quantum Interference Induced Photon Blockade in a Coupled Single Quantum Dot-Cavity System, *Sci. Rep.* **5**, 9252 (2015).
 - [20] X. Y. Liang, Z. L. Duan, Q. Guo, C. J. Liu, S. G. Guan, and Y. Ren, Photon blockade in an atom-cavity system, arXiv:1811.06690 (2018).
 - [21] M. Bamba, A. Imamoglu, I. Carusotto, and C. Ciuti, Origin of strong photon antibunching in weakly nonlinear photonic molecules, *Phys. Rev. A* **83**, 021802(R) (2011).
 - [22] X. W. Xu and Y. Li, Strong photon antibunching of symmetric and antisymmetric modes in weakly nonlinear photonic molecules, *Phys. Rev. A* **90**, 033809 (2014).